HIF1α and HIF2α independently activate SRC to promote melanoma metastases

Sara C. Hanna,[1] Bhavani Krishnan,[1] Sean T. Bailey,[1] Stergios J. Moschos,[1] Pei-Fen Kuan,[1,2] Takeshi Shimamura,[3] Lukas D. Osborne,[4] Marni B. Siegel,[1] Lyn M. Duncan,[5] E. Tim O'Brien III,[4] Richard Superfine,[4] C. Ryan Miller,[1,6] M. Celeste Simon,[7] Kwok-Kin Wong,[8,9] and William Y. Kim[1]

[1]Lineberger Comprehensive Cancer Center and [2]Department of Biostatistics, University of North Carolina at Chapel Hill, Chapel Hill, North Carolina, USA.
[3]Oncology Institute, Department of Molecular Pharmacology and Therapeutics, Loyola University Chicago, Maywood, Illinois, USA.
[4]Department of Physics and Astronomy, University of North Carolina at Chapel Hill, Chapel Hill, North Carolina, USA.
[5]Pathology Service and Dermatopathology Unit, Massachusetts General Hospital, Boston, Massachusetts, USA.
[6]Department of Pathology and Laboratory Medicine, University of North Carolina, Chapel Hill, North Carolina, USA.
[7]Abramson Family Cancer Research Institute, Department of Cancer Biology, Department of Cell and Developmental Biology,
Howard Hughes Medical Institute, University of Pennsylvania, Philadelphia, Pennsylvania, USA. [8]Department of Medicine, Harvard Medical School,
Department of Medical Oncology and Lowe Center for Thoracic Oncology Dana-Farber/Harvard Cancer Center, Boston, Massachusetts, USA.
[9]Ludwig Center at Dana-Farber/Harvard Cancer Center, Boston, Massachusetts, USA.

Malignant melanoma is characterized by a propensity for early lymphatic and hematogenous spread. The hypoxia-inducible factor (HIF) family of transcription factors is upregulated in melanoma by key oncogenic drivers. HIFs promote the activation of genes involved in cancer initiation, progression, and metastases. Hypoxia has been shown to enhance the invasiveness and metastatic potential of tumor cells by regulating the genes involved in the breakdown of the ECM as well as genes that control motility and adhesion of tumor cells. Using a *Pten*-deficient, *Braf*-mutant genetically engineered mouse model of melanoma, we demonstrated that inactivation of HIF1α or HIF2α abrogates metastasis without affecting primary tumor formation. HIF1α and HIF2α drive melanoma invasion and invadopodia formation through PDGFRα and focal adhesion kinase–mediated (FAK-mediated) activation of SRC and by coordinating ECM degradation via MT1-MMP and MMP2 expression. These results establish the importance of HIFs in melanoma progression and demonstrate that HIF1α and HIF2α activate independent transcriptional programs that promote metastasis by coordinately regulating cell invasion and ECM remodeling.

Introduction

Melanoma is one of the most lethal forms of skin cancer and is increasing in incidence (1). Early stage melanomas are highly curable by surgical resection, and adjuvant therapy is rarely necessary. However, patients with later stage melanomas that have progressed to metastasis have a much lower chance of long-term survival (2).

Hypoxia-inducible factor (HIF) is a heterodimeric transcription factor composed of an α and a β subunit. There are 3 α subunit genes: HIF1α, HIF2α, and HIF3α, which partner with a β subunit HIFβ (also known as the arylhydrocarbon nuclear translocator, ARNT) to form a transcriptionally active complex. HIFα subunits are posttranslationally hydroxylated on conserved prolyl residues in an oxygen-dependent manner and then degraded by the von Hippel–Lindau (pVHL) E3 ubiquitin ligase complex, while HIFβ subunits are constitutively stable. Therefore, HIFα subunits are stabilized under hypoxia but degraded under conditions of normoxia (3, 4).

HIF regulates genes that would be predicted to be protumorigenic, including genes involved in adaptation to an unfavorable tumor microenvironment. For example, HIF activates proangio-genic genes, such as *VEGFA*, *PDGFB*, and *IL-8*, genes that regulate cellular pH, such as carbonic anhydrase 9 (*CA9*), and genes that regulate glycolytic cellular metabolism, such as lactate dehydrogenase A (*LDHA*) and phosphofructokinase (*PFK*) (4, 5). While the majority of transcriptional targets of HIF1α and HIF2α are overlapping, it is now clear that HIF1α and HIF2α have unique target genes as well. For example HIF1α specifically regulates multiple genes involved in glycolysis, while HIF2α–specific targets include *OCT4* and cyclin D1 (*CCND1*) among others (6–9).

Hypoxia has been shown to enhance the invasiveness and metastatic capacity of tumor cells and is critical for placental development, a process that requires invasion of the maternal decidua by trophoblast cells (10–13). HIF activation plays a key role in these processes through transcriptional regulation of the following kinds of genes: genes involved in breakdown of the ECM, such as MMPs; genes that are involved in the epithelial-to-mesenchymal transition (EMT), such as E-Cadherin (*CDH1*) and N-Cadherin (*CDH2*); genes that promote metastases, such as *TWIST1* and lysyl oxidase (*LOX*); and genes implicated in motility, adhesion, and invasion, such as *MET/HGF*, *CXCR4/SDF-1*, and αV (*ITGAV*) β3 (*ITGB3*) integrin (4, 5, 13).

Both HIF1α and HIF2α have been shown to be overexpressed in melanoma (14). The dermal-epidermal junction where melanocytes reside is relatively hypoxic, and HIF1α is necessary for the AKT-mediated transformation of melanocytes (15). HIF activation is a consequence of several of the signature genetic events found in melanoma. For example, HIF is upregulated by mutated *Ras* and *Braf* as well as loss-of-function mutations of *PTEN* (16–19). In

addition, HIF appears to mediate a prosurvival signaling pathway downstream of the microphthalmia transcription factor (MITF) (20), but has also been reported to downregulate MITF expression, suggesting a possible negative feedback loop (21, 22). Based on these observations, we sought to directly explore the contributions of HIFs to melanoma pathogenesis. To this end, we studied the impact of Hif1α or Hif2α inactivation on invasion and metastases in vitro as well as in an autochthonous, genetically engineered mouse (GEM) model of melanoma.

Results

Inactivation of Hif1α or Hif2α does not affect the initiation or progression of Braf-activated, Pten-deficient melanomas. For this study, we utilized a previously characterized conditional mouse model of melanoma based on melanocyte-specific *Pten* inactivation and *Braf^V600E* activation (hereafter called *Pten;Braf*) (23). In this model, temporal and spatial expression of Cre recombinase is controlled by tamoxifen and the tyrosinase promoter, respectively. Genetic recombination of floxed alleles therefore occurs in tyrosinase-positive cells exposed to 4-hydroxytamoxifen (4-OHT), giving rise to melanomas that are highly metastatic to regional lymph nodes (23).

To determine whether Hif1α or Hif2α plays an active role in melanoma initiation and progression, we intercrossed *Pten;Braf* mice with mice harboring conditional knockout alleles of *Hif1α* and *Hif2α* (*Hif1^L/L*, hereafter called *Hif1,* and *Hif2^L/L*, hereafter called *Hif2*) to generate cohorts of (a) *Pten;Braf;Hif1*, (b) *Pten;Braf;Hif2*, and (c) *Pten;Braf* control mice. At 6 weeks of age, mice from the above cohorts were treated with topical 4-OHT at the base of the tail to induce recombination of the floxed alleles and initiate tumorigenesis. Pigmented lesions, limited to the site of 4-OHT application, began to appear approximately 3 weeks later (Supplemental Figure 1A; supplemental material available online with this article; doi:10.1172/JCI66715DS1). Upon tumor formation, validation of Hif1α or Hif2α loss was confirmed by Western blot of tumor lysates (Supplemental Figure 1B). However, neither inactivation of *Hif1α* nor of *Hif2α* appeared to affect melanoma pigmentation grossly (Figure 1A), their growth rate relative to control *Pten;Braf* tumors (Supplemental Figure 1C), or the percentage of mice living (mice were sacrificed secondary to primary tumor burden) (Figure 1B). Moreover, inactivation of *Hif1α* or *Hif2α* in *Pten;Braf* melanomas did not appear to alter the tumor-free survival of the mice harboring these tumors (Supplemental Figure 1D) nor the weight of the tumor itself (Supplemental Figure 1E). In aggregate, these data suggest that Hif1α and Hif2α are dispensable for the initiation and progression of *Pten;Braf* melanomas.

Histological analysis confirmed that inactivation of Hif1α or Hif2α in *Pten;Braf* melanomas did not appreciably alter their pigmentation and that the tumors were virtually indistinguishable (Figure 1A). The melanomas continued to have a dense stroma and reside at the epidermal-dermal junction consistent with previous observations (23). Constitutive expression of Hif1α and Hif2α (due to inactivation of pVHL) is intimately associated with the pathogenesis of renal cell carcinoma (RCC), and in this context as well as that of other solid tumors, Hif1α and Hif2α activation potently stimulates angiogenesis (4, 24). We therefore also examined the effects of Hif1α or Hif2α inactivation on the vascularity of *Pten;Braf* melanomas. Loss of Hif1α or Hif2α decreased melanoma vascularity (as assessed by the number of CD31+ microvessels per high powered field) of *Pten;Braf;Hif1* and *Pten;Braf;Hif2* melanomas relative to *Pten;Braf* controls (Supplemental Figure 1, F and G).

Thus, while Hif1α and Hif2α regulate melanoma angiogenesis, this did not have an impact on melanoma growth.

HIF1α and HIF2α expression are increased in melanoma metastases and their inactivation abrogates lymph node metastases of Pten;Braf melanomas. Both expression of HIF and tumor hypoxia correlate with an increased rate of metastases in many tumor types (11, 19). We therefore hypothesized that, while Hif1α and Hif2α do not play prominent roles in melanoma initiation or progression, they might have an impact on its metastatic capacity.

To explore this possibility, tissue microarrays (TMAs) spotted with nevi, thin (Breslow thickness of invasion ≤ 2 mm) and thick primary melanomas, and melanoma metastases were stained with antibodies specific to HIF1α and HIF2α and scored in a blinded fashion (Figure 1, C and D). While HIF1α had a progressive increase in expression from nevus to metastasis, HIF2α expression was more variable, with the high levels of expression seen in thick primary melanomas as well as metastases.

Examination of the regional lymph nodes in *Pten;Braf* mice revealed significant areas of pigmentation (Figure 1E, gross) as previously described in this model (23). In contrast, the locoregional lymph nodes from mice harboring *Pten;Braf;Hif1* and *Pten;Braf;Hif2* melanomas either had markedly fewer foci or completely lacked visible pigmentation, suggesting that deletion of *Hif1α* or *Hif2α* may abrogate lymph node metastases.

Histologic examination of the lymph nodes from mice harboring *Pten;Braf* melanomas confirmed the presence of clusters of melanin pigment–positive melanoma cells in the subcapsular sinuses of lymph nodes, indicative of melanoma metastases (Figure 1E, ×10 and ×20). However, examination of lymph nodes from *Pten;Braf;Hif1* and *Pten;Braf;Hif2* mice showed a relative absence of these melanotic foci. Quantification of lymph node metastases revealed that mice with *Pten;Braf* melanomas had a significantly higher percentage of lymph node metastases than mice harboring *Pten;Braf;Hif1* and *Pten;Braf;Hif2* melanomas (Figure 1F) as well as a higher percentage of melanin per lymph node (Supplemental Figure 1H). Detailed histologic assessment confirmed that HIF deficiency did not simply result in loss of pigmentation in the metastasis or result in a different pattern of metastatic spread. Therefore, Hif1α and Hif2α are required for lymphatic metastases in *Pten;Braf* melanomas.

Hypoxia enhances melanoma cell invasion and invadopodia formation. Previous work has shown that melanoma cell lines expressing mutant *BRAF^V600E* express detectable levels of HIF1α under normoxia (16). We wished to examine HIF1α or HIF2α expression in human melanoma cells in comparison with human neonatal foreskin melanocytes under conditions of normoxia or hypoxia. To this end, a panel of *BRAF^V600E* mutant melanoma cell lines or nontransformed melanocytes was cultured in normoxia (21% O_2) or hypoxia (1% O_2) overnight. Whole-cell extracts were then immunoblotted for HIF1α or HIF2α (Figure 2A). Most melanoma cell lines displayed variable levels of both HIF1α and HIF2α in hypoxia. While there were detectable levels of HIF1α in cells cultured under normoxia (Supplemental Figure 2), they were significantly lower than those found in hypoxia, and we did not see appreciable levels of normoxic HIF2α.

Hypoxia reportedly increases the invasiveness of cancer cells and trophoblast stem cells (TS cells) in certain physiologic contexts in vitro. This hypoxia-induced invasion is reduced by deletion of ARNT or coinactivation of Hif1α and Hif2α (13). However, whether inactivation of HIF1α or HIF2α alone was sufficient to
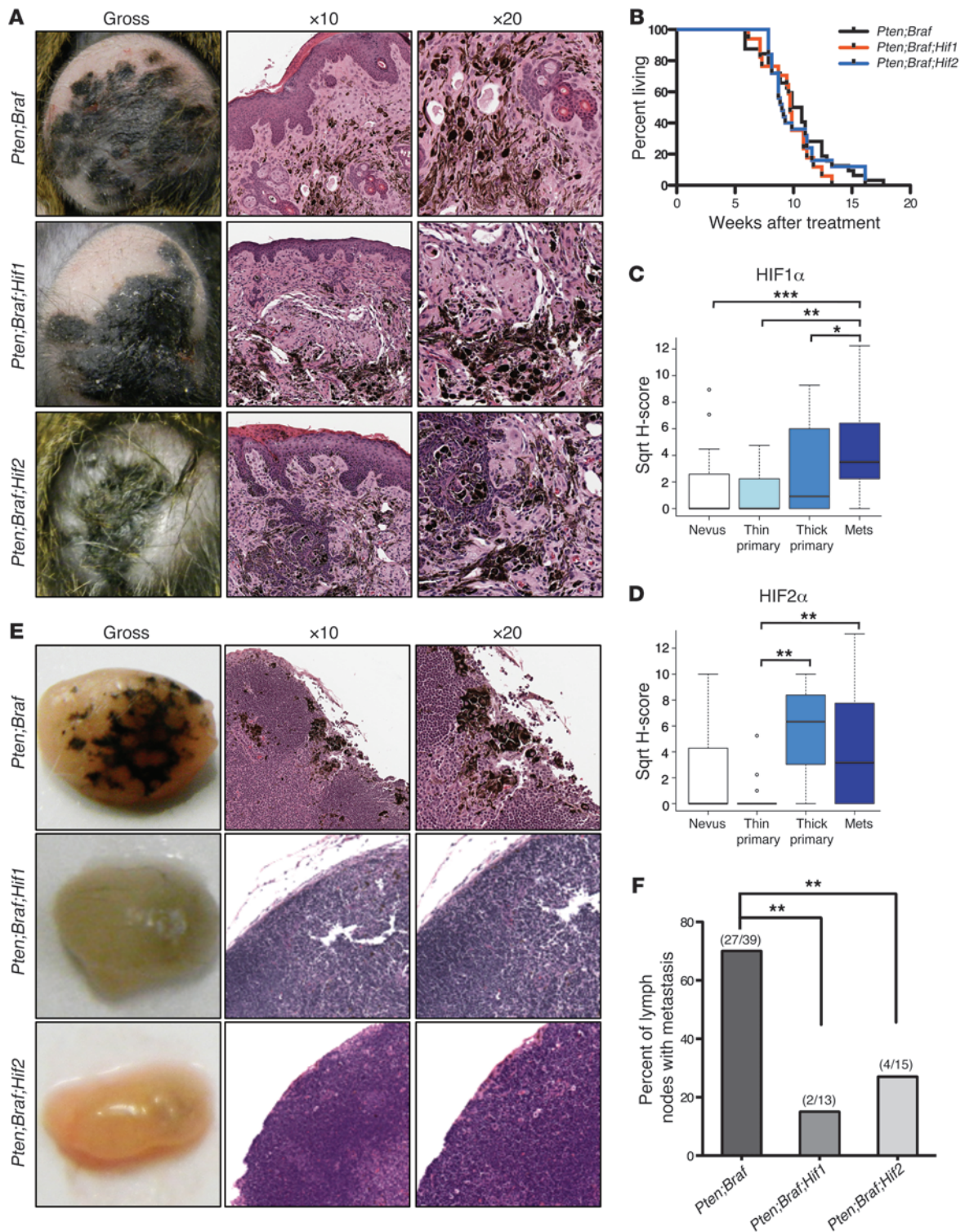
Figure 1
Inactivation of Hif1α or Hif2α does not affect initiation of the survival or growth of *Pten;Braf* melanomas, but abrogates lymph node metastases. (**A**) Representative gross images as well as low- and high-power photomicrographs of H&E-stained *Pten;Braf*, *Pten;Braf;Hif1*, and *Pten;Braf;Hif2* melanomas taken at gross, ×10, and ×20 magnification. (**B**) Kaplan-Meier survival curve of cohorts of mice of the indicated genotypes (*Pten;Braf*, n = 39; *Pten;Braf;Hif1*, n = 20; and *Pten;Braf;Hif2*, n = 28). P = 0.6585, log-rank test. (**C** and **D**) TMA analysis of HIF1α and HIF2α expression in melanocytic lesions. (**E** and **F**) Representative gross images, low- and high-power photomicrographs, and quantification of lymph node metastases from the indicated genotypes *Pten;Braf* (27/39), *Pten;Braf;Hif1* (2/13), and *Pten;Braf;Hif2* (4/15) taken at gross, ×10, and ×20 magnification. Error bars show SEM. ***P < 0.0005; **P < 0.005; *P < 0.05.
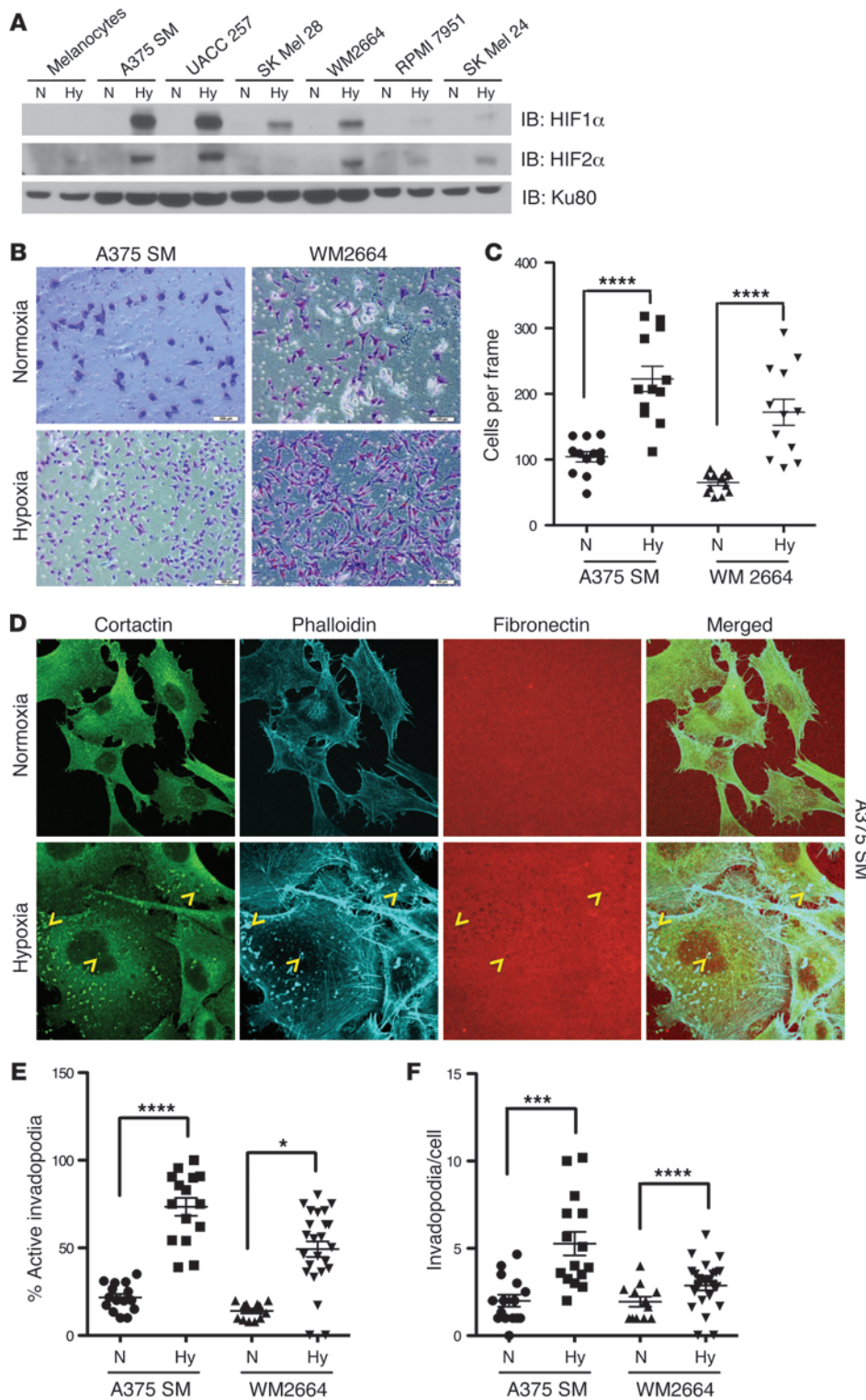
decrease invasion was not examined. We first wanted to confirm that hypoxia could induce the invasion of melanoma cells through Matrigel. To this end, A375 SM and WM2664 cells were allowed to invade a Matrigel chamber under both normoxia and hypoxia. Hypoxia significantly increased the number of cells invading the Matrigel chamber in both cell lines (Figure 2, B and C) and

also appeared to increase melanoma cell motility (Supplemental Figure 3, A and B) in an in vitro wound closure assay. Therefore, consistent with previously published results in other tumor types, hypoxia increases cell motility and invasion of melanoma cells.

Invadopodia are dynamic, actin-rich protrusions of the cellular membrane that are points of both ECM degradation and attach-

A A375 SM   WM2664

IB: HIF1α
IB: HIF2α
IB: Ku80

1% O₂

B siNS   siHIF1α   siHIF2α

A375 SM

WM2664

1% O₂

C
Cells per frame

A375 SM   WM2664

1% O₂

D Cortactin   Phalloidin   Fibronectin   Merged

siNS

siHIF1α

siHIF2α

A375 SM 1% O₂

E
% Active invadopodia

A375 SM   WM2664

1% O₂

F
Lung mets per mouse

A375 SM

G shNS   shHIF1α   shHIF2α

Ventral

Posterior
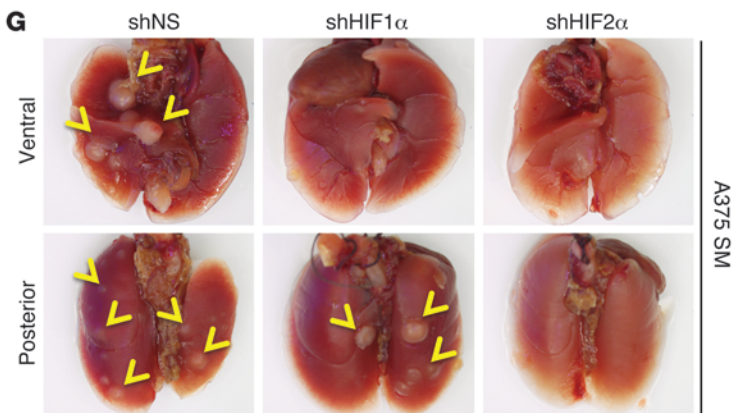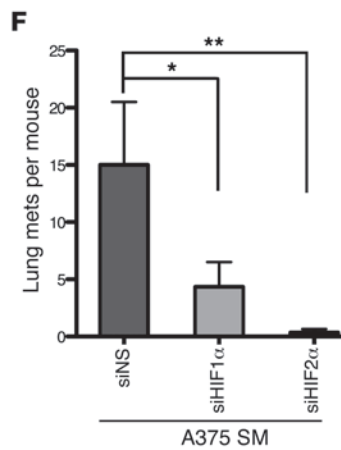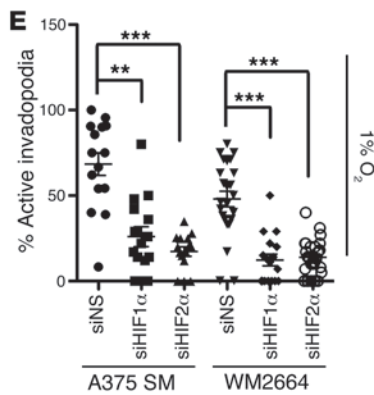
A375 SM

Figure 3

Knockdown of HIF1α or HIF2α reduces the hypoxia-induced invasion and invadopodia formation of melanoma cell lines. (**A**) A375 SM and WM2664 cells were transfected with siRNAs against HIF1α, HIF2α, or a nonspecific sequence (NS). Whole-cell lysates were immunoblotted with the indicated antibodies. (**B**) Representative photomicrographs of A375 SM and WM2664 cells transfected with the indicated siRNAs, which have invaded through Matrigel chambers under hypoxia. Original magnification, ×10. (**C**) Quantification of A375 SM and WM2664 cells transfected with the indicated siRNAs, which have invaded through Matrigel chambers under hypoxia. (**D**) Representative immunofluorescence images of siRNA-transfected A375 SM cells plated on Alexa Fluor 568–conjugated fi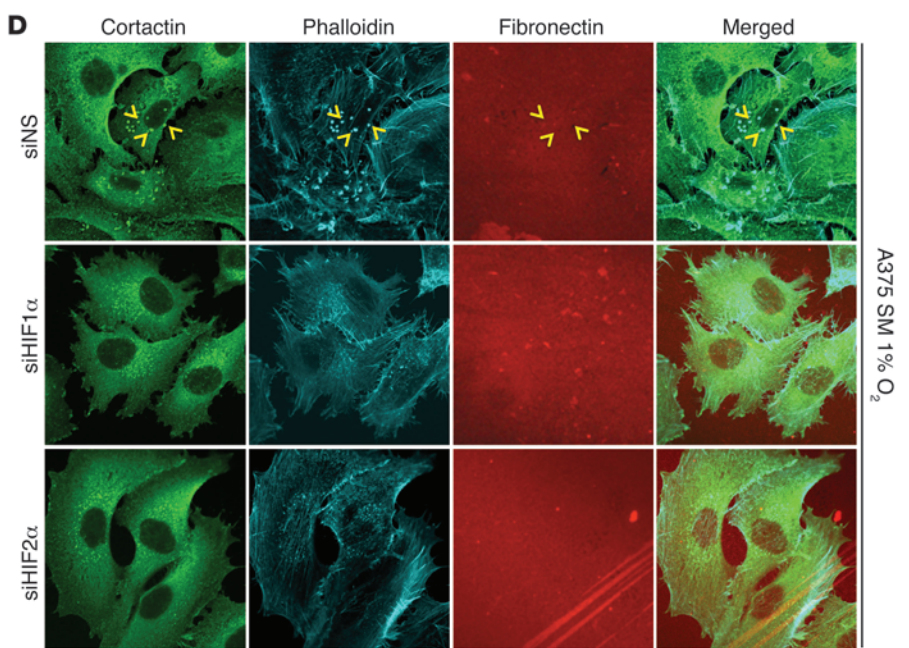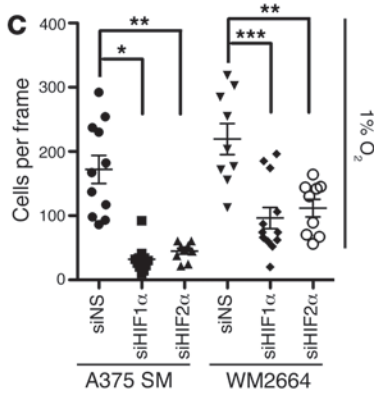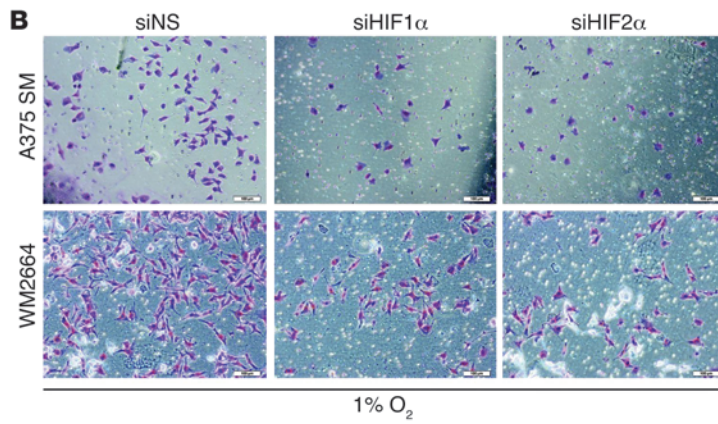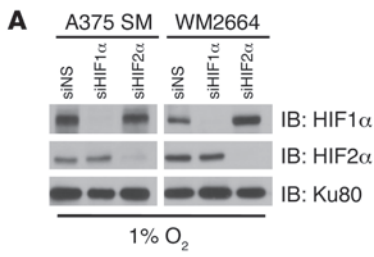bronectin and stained with the indicated antibodies. Original magnification, ×63. Invadopodia were defined as colocalization of cortactin, F-actin (phalloidin), and degradation of Alexa Fluor 568 fibronectin and are indicated with yellow arrowheads. (**E**) Quantification of the percentage of cells with active invadopodia in siRNA-transfected A375 SM and WM2664 cells. (**F**) Quantification of the number of visible lung metastases found in mice tail vein injected with A375 SM cells. (**G**) Gross representative images of the lungs from tail-vein–injected mice. Yellow arrows indicate lung metastases. Error bars show SEM. ***$P < 0.0005$; **$P < 0.005$; *$P < 0.05$.

ment (25). Invadopodia coordinate ECM degradation with cell motility and correlate highly with cancer cell invasiveness. Given this relationship between invadopodia and tumor cell invasion, we determined whether hypoxia could induce invadopodia formation in melanoma cell lines. A375 SM and WM2664 cells were plated on Alexa Fluor 568–labeled fibronectin (artificial ECM) and allowed to form invadopodia in either normoxia or hypoxia overnight. Melanoma cells cultured under hypoxia had significantly more cells with active invadopodia (defined as colocalization of F-actin [phalloidin staining] and cortactin punctae with degradation of fibronectin) as well as a higher number of invadopodia per cell (Figure 2, D–F). In aggregate, these data suggest that hypoxia promotes melanoma invasiveness as well as the formation of active invadopodia.

Hypoxia-induced invasion and invadopodia formation are dependent upon HIF1α or HIF2α. We next asked whether either HIF1α or HIF2α was necessary for hypoxia-induced invasion and invadopodia formation of melanoma cell lines. siRNAs directed to HIF1α and HIF2α were effective and specific at knocking down HIF1α and HIF2α in A375 SM and WM2664 cells cultured in hypoxia (Figure 3A). While HIF1α or HIF2α knockdown did not appreciably affect cell proliferation or survival, they both affected multiple parameters of cell motility and invasion relative to cells expressing nonspecific siRNAs. These included decreases in cellular migration under hypoxia (Supplemental Figure 3, C and D) but not normoxia (Supplemental Figure 3, E and F), Matrigel invasion (Figure 3, B and C, and Supplemental Figure 4, A and B), and invadopodia formation (Figure 3, D and E, and Supplemental Figure 4C). Therefore, the increased invasiveness and numbers of invadopodia induced by hypoxia are both HIF1α and HIF2α dependent. Finally, to assess the functional relevance of these in vitro outcomes, we stably silenced HIF1α or HIF2α and assessed these cells' ability to form tumors upon tail-vein injection. shRNA to HIF1α or HIF2α significantly decreased the number of lung metastases after tail-vein injection of A375 SM cells (Figure 3, F and G). Therefore, the in vitro decrease in motility, invasion, and invadopodia formation induced by silencing of HIF1α or HIF2α are reflected in in vivo metastatic tumor formation.

HIF1α and HIF2α upregulate PDGFRα and FAK and are necessary for hypoxia-induced SFK activation. Invadopodia were first described in chicken fibroblasts and were notably increased in fibroblasts transformed with viral-SRC (v-SRC) (25). It is now clear that SRC activation is a critical step in invadopodia formation. While various physiologic and pathogenic stimuli have been shown to upregulate SRC activity, only a few reports have examined whether hypoxia can result in SRC activation (26). We confirmed that SRC family kinases (SFK) could be activated by hypoxia by immunoblotting A375 SM and WM2664 cells with an antibody that recognizes phosphorylated Tyr416 within the activation loop of the cellular SRC (c-SRC) or its equivalent site on the other SFK members (Lyn, Fyn, Lck, Yes, and Hck) (Figure 4A). In keeping with the notion that hypoxia-induced phosphorylation of SFK$_{Tyr416}$ is dependent upon HIF1α or HIF2α, knockdown of HIF1α or HIF2α under hypoxia or deletion of Hif1α or Hif2α in *Pten;Braf* melanomas significantly decreased levels of SFK$_{Tyr416}$ (Figure 4, B and C). Importantly, silencing of HIF1α or HIF2α did not appear to alter total SRC protein levels, suggesting that HIF1α and HIF2α RNAi were not merely decreasing total SRC expression, but were specifically regulating SRC activity (Figure 4, B and C).

Since HIF1α and HIF2α are transcription factors, we predicted that SFK activation is mediated through one or more of their transcriptional targets. In this regard, *TWIST1*, a well characterized HIF target gene, was recently shown to promote invadopodia formation and metastases via a PDGFRα-dependent upregulation of SFK in breast cancer cells (27–29). We therefore asked whether HIF1α and/or HIF2α regulate TWIST1 or PDGFRα in melanoma cells. We found that siRNA of HIF1α (but not HIF2α) specifically downregulated *PDGFRA* mRNA and protein levels under hypoxia in melanoma cell lines (Figure 4, B and D) and that inactivation of Hif1α (but not Hif2α) decreased *Pdgfra* mRNA expression in primary tumors (Supplemental Figure 5A). Unexpectedly, *TWIST1* expression was unaffected (Supplemental Figure 5, C and D).

Since our data indicate that HIF2α regulates pSFK through a pathway distinct from the HIF1α-PDGFRα axis, we examined whether HIF2α regulates expression of focal adhesion kinase (FAK), an activator of SRC (26). Correspondingly, siRNA of HIF2α (but not HIF1α) under hypoxia specifically downregulated both *FAK* mRNA and protein levels (Figure 4, B and E) and *Fak* mRNA expression was decreased in *Pten;Braf* melanomas with Hif2 inactivation (Supplemental Figure 5B). Moreover, ChIP with antibodies specific to HIF1α and HIF2α demonstrated that both HIF1α and HIF2α were recruited to the promoter regions of *PDGFRA* and *FAK* in a hypoxia-dependent manner (Supplemental Figure 5, E–H). At first approximation, this would seem contrary to the results showing that HIF1α and HIF2α specifically regulate PDGFRα and FAK. However, these results are in keeping with previous studies that have shown that recruitment of transcriptional coactivators rather than promoter occupancy determines HIF target gene specificity (30).

Finally, concurrent knockdown of HIF1α and HIF2α in the same cell resulted in an additive decrease of pSFK (Figure 4F) as well as Matrigel invasion (Figure 4, G–I). In aggregate, these data show that hypoxia activates SRC in a manner dependent upon both HIF1α and HIF2α, which act via parallel yet distinct signaling programs involving PDGFRα and FAK, respectively.

Expression of stabilized HIF1α or HIF2α is sufficient to enhance normoxic melanoma cell invasion, invadopodia, and reduce cell stiffness. While the above data suggest that HIF1α and HIF2α are necessary for hypoxia-dependent activation of SFK, invadopodia formation,
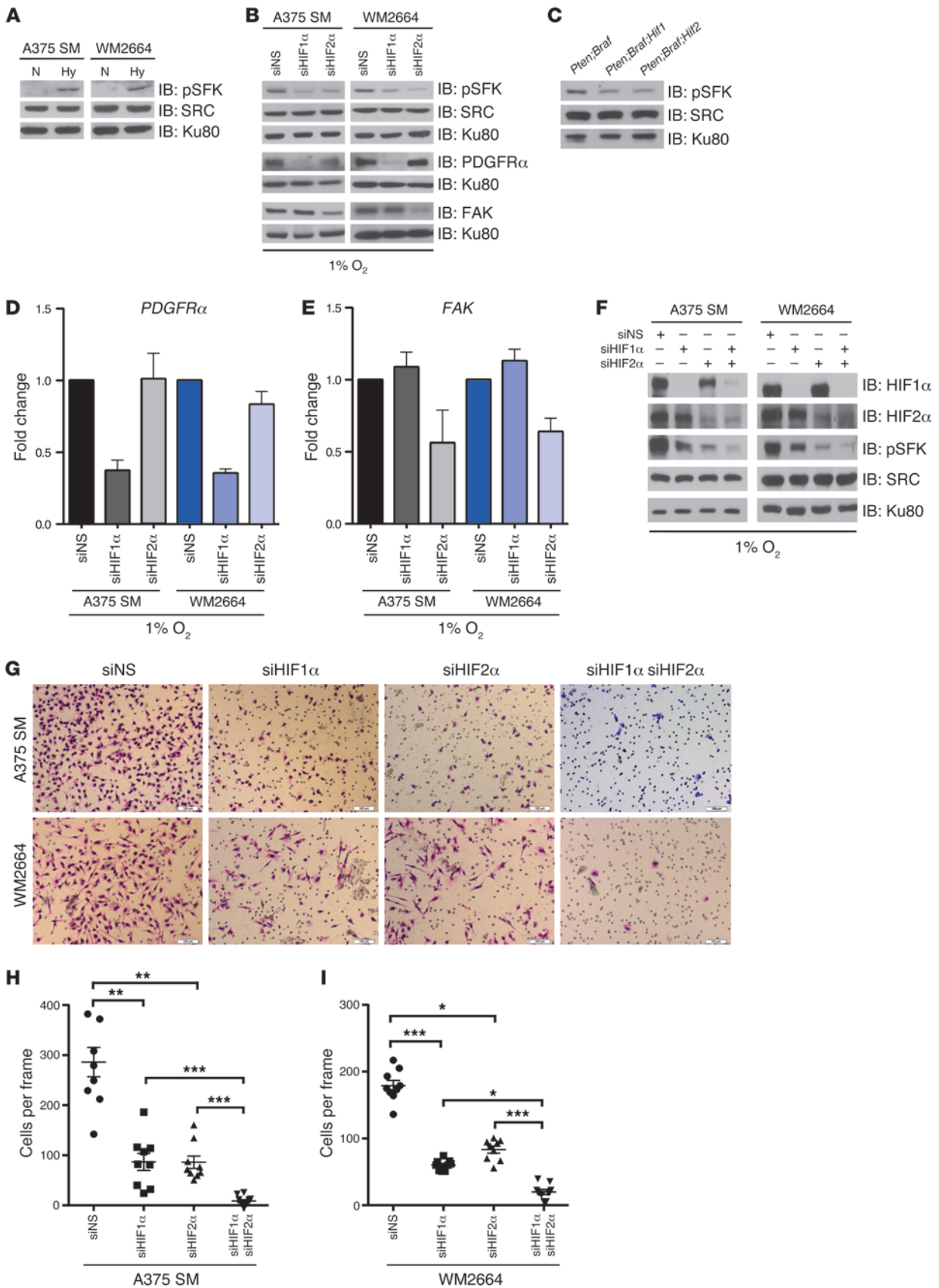
Figure 4

HIF1α and HIF2α upregulate PDGFRα and FAK and are necessary for hypoxia-induced SFK activation. (**A**) A375 SM and WM2664 cells were cultured in normoxia (21% O₂) or hypoxia (1% O₂) overnight. Whole-cell extracts were immunoblotted with the indicated antibodies. (**B**) A375 SM and WM2664 cells were transfected with siRNAs against HIF1α, HIF2α, or a nonspecific sequence. Whole-cell lysates were immunoblotted with the indicated antibodies. (**C**) Tumor lysates from the indicated cohorts were immunoblotted for the indicated antibodies. (**D** and **E**) A375 SM and WM2664 cells were transfected with siRNAs against HIF1α, HIF2α, or a nonspecific sequence and cultured under hypoxia overnight. Total RNA was used to perform TaqMan quantitative real-time PCR for *PDGFRA* and *FAK*. (**F**) A375 SM and WM2664 cells were transfected with siRNAs against HIF1α, HIF2α, both HIF1α and HIF2α, or a nonspecific sequence. Whole-cell lysates were immunoblotted with the indicated antibodies. (**G**) Representative photomicrographs of A375 SM and WM2664 cells transfected with the indicated siRNAs, which have invaded through Matrigel chambers. Original magnification, ×10. (**H** and **I**) Quantification of A375 SM and WM2664 cells transfected with the indicated siRNAs, which have invaded through Matrigel chambers. Error bars show SEM. ***$P < 0.0005$; **$P < 0.005$; *$P < 0.05$.

and invasion, we wanted to determine whether HIF1α and HIF2α were sufficient to mediate these cellular signaling events and phenotypes. To this end we generated A375 SM and WM2664 cells expressing stabilized versions of HIF1α and HIF2α (HIF1dPA and HIF2dPA) that remain stable under normoxia (ref. 31 and Figure 5A). Importantly, the HIF1α- and HIF2α-expressing cells exhibited increases in melanoma cell line invasion (Figure 5, B and C) and invadopodia formation (Figure 5, D and E, and Supplemental Figure 6). Additionally, HIF2dPA and to a lesser extent HIF1dPA were sufficient to increase pSFK levels (Figure 5F). The reduced potency of HIF1dPA may reflect the residual sensitivity of this isoform to proteasome inhibition and consequent lower levels of expression (6). Nonetheless, cells expressing HIF1dPA had increased levels of PDGFRα, while those expressing HIF2dPA had increased expression of FAK (Figure 5F), suggesting that expression of HIF1α and HIF2α are sufficient for the normoxic upregulation of PDGFRα and FAK respectively.

Previous work has identified physical properties such as cell stiffness as correlating with the invasive ability of cancer cells (32–34), and a variety of biophysical techniques including "magnetic tweezers" allow for measurements of cell stiffness in living cells. To determine whether the increased invasiveness associated with expression of stabilized HIF1α or HIF2α also correlated with alterations in cell compliance, fibronectin-conjugated magnetic beads were first allowed to associate with A375 SM cells expressing EGFP, HIF1dPA, or HIF2dPA, a magnetic pulse was then applied to each bead, and the resultant motion and recovery of the bead position were used to calculate cell stiffness (expressed in pascals [Pa]), as previously described (Figure 5G and ref. 33). An extracellular passive microrheology assay was also conducted and obtained measurements of cell stiffness that confirmed these findings (Supplemental Figure 7, A and B; ref. 35). These results demonstrate that not only are HIF1α and HIF2α sufficient to increase cell invasiveness, but they also significantly decrease cell stiffness.

HIF1α- and HIF2α-induced invasion is dependent on PDGFRα and FAK, respectively. In order to determine whether HIFα-induced invasion is dependent on PDGFRα or FAK, we assessed the effect of silencing PDGFRα or FAK on the invasive ability of A375

SM and WM2664 cells expressing stabilized versions of HIF1α or HIF2α. To this end, we first verified efficient knockdown of PDGFRα or FAK in cells expressing stabilized HIF1α or HIF2α (Figure 6A). In keeping with the model that HIF1α and HIF2α specifically regulate PDGFRα and FAK, respectively, we saw that knockdown of PDGFRα resulted in decreased pSFK only in cells expressing stabilized HIF1α, while knockdown of FAK decreased pSFK in cells expressing stabilized HIF2α (Figure 6A). Moreover, consistent with the notion that HIF1α- and HIF2α-induced invasion are specifically dependent upon PDGFRα and FAK, respectively, knockdown of PDGFRα selectively inhibited the invasive ability of the melanoma cell lines expressing HIF1dPA (Figure 6, B–D), while knockdown of FAK only inhibited the invasive ability of the melanoma cell lines expressing HIF2dPA (Figure 6, B–D). In addition, consistent with the model that both HIF1α and HIF2α mediate their invasive effects via SRC, we noted that SRC inhibition with dasatinib (100 nM) was sufficient to block the invasion of A375 SM and WM2664 cells expressing stabilized HIF1α or HIF2α (Supplemental Figure 8, A–C). These data in aggregate demonstrate that PDGFRα is responsible for HIF1α-mediated invasion while HIF2α mediates invasion through FAK and that both HIF1α and HIF2α require SRC for invasion.

HIF1α and HIF2α regulate expression of MMPs implicated in invadopodia formation. One of the primary features that distinguish invadopodia from other plasma membrane protrusions such as filopodia or lamellipodia is the ability to degrade the ECM (25). This focal ECM degradation (primarily mediated by MMPs) allows the coordinated destruction of the ECM with cellular motility and invasion. In this regard, both a membrane-bound MMP, MT1-MMP (membrane type 1 MMP, also known as MMP14), and secreted MMPs, MMP2 and MMP9 colocalize with active invadopodia and are key determinants of invadopodia formation (25). We found that endogenous HIF1α was necessary for the hypoxic expression of MT1-MMP and that HIF1dPA could directly enhance normoxic MT1-MMP expression. In contrast, manipulations of HIF2α failed to alter MT1-MMP levels (Figure 7, A–C), but specifically regulated MMP2 expression (Figure 7, A, B, and D). Therefore, HIF1α and HIF2α not only regulate SRC activation, but also the expression of key MMPs involved in invadopodia-associated ECM degradation.

To address whether the regulation of MT1-MMP and MMP2 by HIF1α and HIF2α had a functional effect on melanoma invasion, we performed RNAi against MT1-MMP or MMP2 in our cell lines expressing stabilized HIF1α (HIF1dPA) and HIF2α (HIF2dPA) (Figure 7E). We had hypothesized that knockdown of MT1-MMP or MMP2 would decrease HIF1α- and HIF2α-mediated invasion, respectively. Unexpectedly, knockdown of either MT1-MMP or MMP2 resulted in a decrease of both HIF1α- and HIF2α-mediated invasion. (Figure 7, F–H). These results suggest that, while HIF1α and HIF2α are necessary and sufficient to regulate MT1-MMP and MMP2, respectively, the levels of MT1-MMP and MMP2 seen under normoxia (Figure 7B) are adequate to mediate invasion.

Knockdown of Hif1α and Hif2α reduces the hypoxia-induced invasion of cell lines derived from Pten;Braf murine melanomas. Collectively, our data demonstrate that HIF1α and HIF2α regulate a transcriptional program of genes involved in the formation of active invadopodia, cancer cell invasion, and cellular stiffness. To determine whether Hif1α and Hif2α behaved similarly in a defined genetic background, we generated cell lines from 2 independent *Pten;Braf* melanomas (2130 and 2460). The cells expressed Tryp1 protein (Supplemental Figure 9A) and had deletion of exons 4 and 5 of
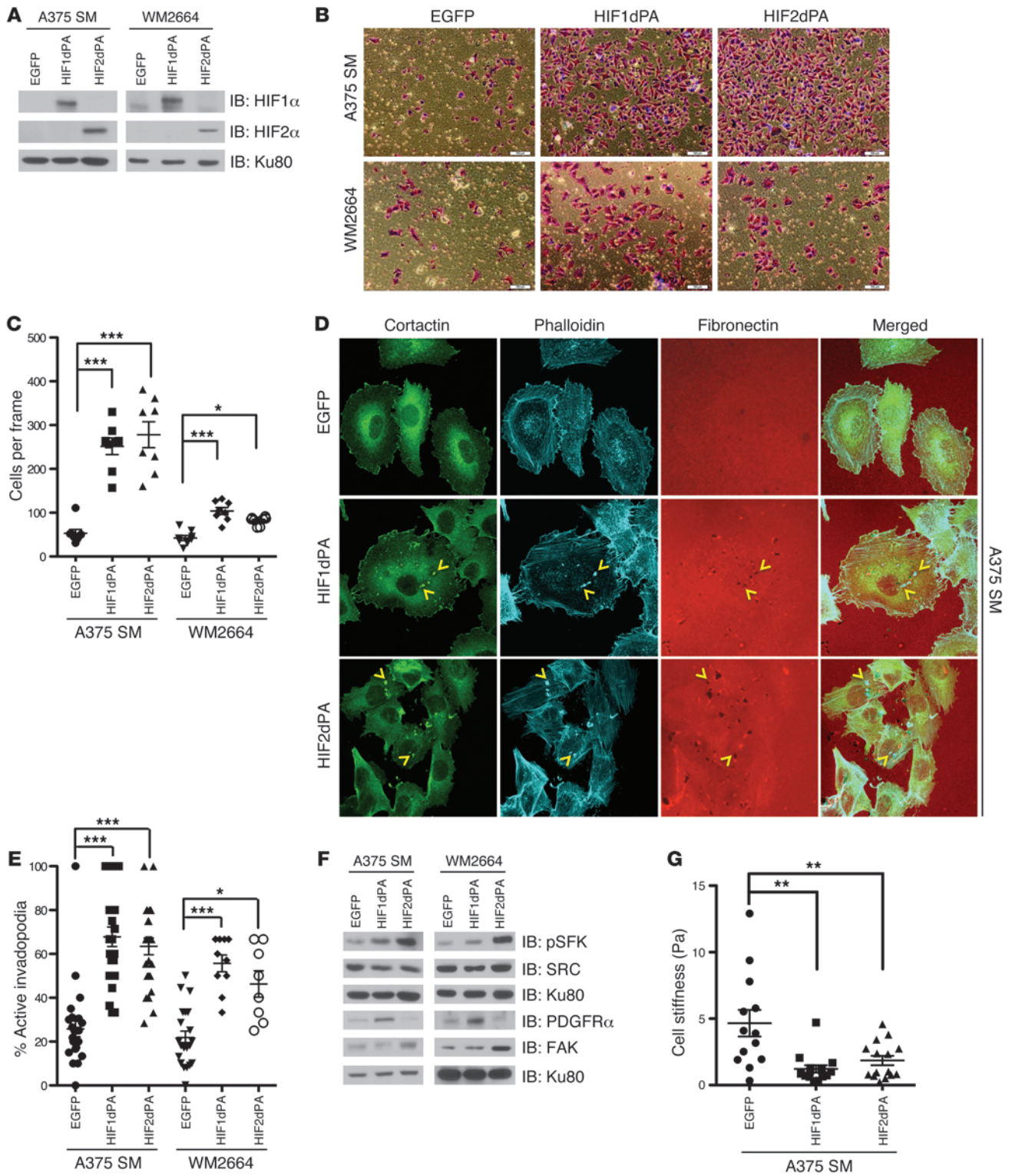
Figure 5

Expression of stabilized HIF1α and HIF2α are sufficient to enhance normoxic melanoma cell invasion. (**A**) A375 SM and WM2664 cells were infected with retrovirus to stably express EGFP or stabilized versions of HIF1α (HIF1dPA) or HIF2α (HIF2dPA). Whole-cell extracts were immunoblotted with the indicated antibodies. (**B**) Representative photomicrographs of A375 SM and WM2664 cells stably expressing EGFP, HIF1dPA, or HIF2dPA, which have invaded through Matrigel chambers. Original magnification, ×10. (**C**) Quantification of A375 SM and WM2664 cells stably expressing EGFP, HIF1dPA, or HIF2dPA, which have invaded through Matrigel chambers. (**D**) Representative immunofluorescence images of A375 SM cells stably expressing EGFP, HIF1dPA, or HIF2dPA and plated on Alexa Fluor 568–conjugated fibronectin and stained with the indicated antibodies. Original magnification, ×63. Invadopodia were defined as colocalization of cortactin, F-actin (phalloidin), and degradation of Alexa Fluor 568 fibronectin and are indicated with yellow arrowheads. (**E**) Quantification of the percentage of cells with active invadopodia in A375 SM and WM2664 cells stably expressing EGFP, HIF1dPA, or HIF2dPA. (**F**) Whole-cell extracts from A375 SM and WM2664 cells stably expressing EGFP, HIF1dPA, or HIF2dPA were immunoblotted with the indicated antibodies. (**G**) A375 SM cells stably expressing EGFP, HIF1dPA, or HIF2dPA were allowed to adhere to fibronectin-conjugated magnetic beads and subjected to repeated magnetic pulses; the resultant motion and recovery were quantified and used to calculate cell stiffness in Pascals (Pa). Error bars show SEM. ***$P < 0.0005$; **$P < 0.005$; *$P < 0.05$.

Pten (Supplemental Figure 9B), suggesting that they were derived from melanocyte lineage and had also undergone TyrCre[ERT2]-mediated recombination respectively.

Loss of PTEN and activation of BRAF are expected to result in increased levels of HIF1α as a consequence of PI3K and MEK/ERK upregulation, respectively (16–19). In keeping with this notion, we saw that pharmacologic inhibition of either BRAF or PI3K with vemurafenib and PIK90, respectively, downregulated not only HIF1α but also HIF2α levels (Figure 8A), suggesting that these oncogenic pathways contribute to the activation of HIF1α and HIF2α under conditions of hypoxia.

Finally, consistent with the findings in our human melanoma cell lines, hypoxia significantly increased the invasiveness of the *Pten;Braf* melanoma cell lines (2130 and 2460) through Matrigel (Figure 8, B and C). Moreover, knockdown of *Hif1α* and *Hif2α* was sufficient to decrease the hypoxic invasion of *Pten;Braf* melanoma cell lines (Figure 8, D–F). These results therefore substantiate the conclusion that Hif1α and Hif2α are necessary for hypoxia-induced invasion in a defined genetic background of melanoma cell lines derived from murine *Pten;Braf* tumors.

Discussion

We found that while inactivation of Hif1α or Hif2α did not affect the initiation or progression of *Pten;Braf* melanomas, it significantly reduced the incidence of lymphatic metastases (Figure 1F). Consistent with these findings, we show that HIF1α and HIF2α expression are increased in thick melanomas and metastases from patients and are both necessary and sufficient for the invasion and invadopodia formation of melanoma cell lines. Moreover, HIF1α and HIF2α activate distinct transcriptional programs that converge to activate SRC and coordinate ECM degradation via PDGFRα/MT1-MMP and FAK/MMP2, respectively. Finally, we demonstrate that hypoxia activates SRC and increases the invasiveness of cell lines derived from *Pten;Braf* melanomas and that hypoxia-induced invasion of these cells can be abrogated by knock-

down of Hif1α or Hif2α. Collectively, these findings demonstrate that, while HIF1α and HIF2α do not have an impact on primary melanoma initiation or progression, they promote melanoma cell invasion, invadopodia formation, and metastases through distinct yet convergent transcriptional programs.

Previous work examining the angiogenic profile of malignant melanomas shows that a significant percentage of human melanomas express detectable levels of HIF1α and HIF2α by immunohistochemistry, but that only levels of HIF2α correlate with VEGF expression and a poor prognosis (14). Other work has confirmed that both mouse and human skin is relatively hypoxic and that, at least in the context of *Ink4a/Arf*-deficient mouse melanocytes, hypoxia and specifically stabilized HIF1α can cooperate with constitutively active AKT in transformation (15). Whether HIF2α can mediate a similar effect was not determined. In our own studies, we stained a TMA from a large sample of patients with a spectrum of melanocytic lesions ranging from benign nevi to metastatic melanomas and showed that both HIF1α and HIF2α expression are increased in thick primary melanomas and metastases. In addition, we determined whether either loss of Hif1α or Hif2α affected the initiation of *Pten;Braf* melanomas in GEM models. We found that inactivation of *Hif1α* or *Hif2α* did not affect either tumor formation or the rate of melanoma growth after their formation. While there are distinct differences in the systems utilized (i.e., soft agar assays and xenografts versus an in vivo autochthonous model) as well as the genetic background of the cells (i.e., constitutively activated Akt and Ink4a/Arf deletion versus Pten loss and mutant Braf activation), our results suggest that, at least in a GEM model of melanoma initiated by *Pten* loss and *Braf* activation, inactivation of Hif1α or Hif2α did not appreciably affect melanocyte transformation or melanoma progression.

Our in vitro studies in both human melanoma cell lines and the cell lines derived from *Pten;Braf* murine melanomas suggest that HIF1α and HIF2α are critical nodes that mediate the hypoxia-induced motility and invasiveness of melanoma cells. This work delineates the pathways activated by HIF1α and HIF2α that mediate actin nucleation and ECM degradation at the forefront of invadopodia and shows for what we believe is the first time that HIF1α and HIF2α are necessary and sufficient for invadopodia formation. Notably, our data indicate what we believe to be a novel paradigm, that HIF1α and HIF2α act to promote a metastatic program through distinct pathways. Specifically, HIF1α induces SRC activity and ECM degradation via PDGFRα and MT1-MMP, while HIF2α signals to SRC via FAK and promotes ECM remodeling through MMP2. Therefore, the transcriptional suite of genes activated by HIF1α and HIF2α in response to hypoxia coordinates the 2 processes that define invadopodia: (a) actin nucleation at cell membrane protrusions and (b) expression of proteases involved in the degradation of the ECM (25). Moreover, these HIF-dependent increases in invasion and invadopodia formation are accompanied by decreases in cell stiffness, a physical property of cells that has been previously shown to inversely correlate with the invasive capacity of cells (32–34). Whether these HIF-induced alterations in cell compliance are a result of the same signaling pathways affecting HIF-induced invasion has yet to be determined.

There are striking clinical similarities between malignant melanoma and RCC, including their hypervascularity and propensity for hemorrhagic central nervous system metastases, relative resistance to radiation therapy, and, most intriguingly, their responsiveness to immunomodulatory agents such as IL-2, INF-α, and,
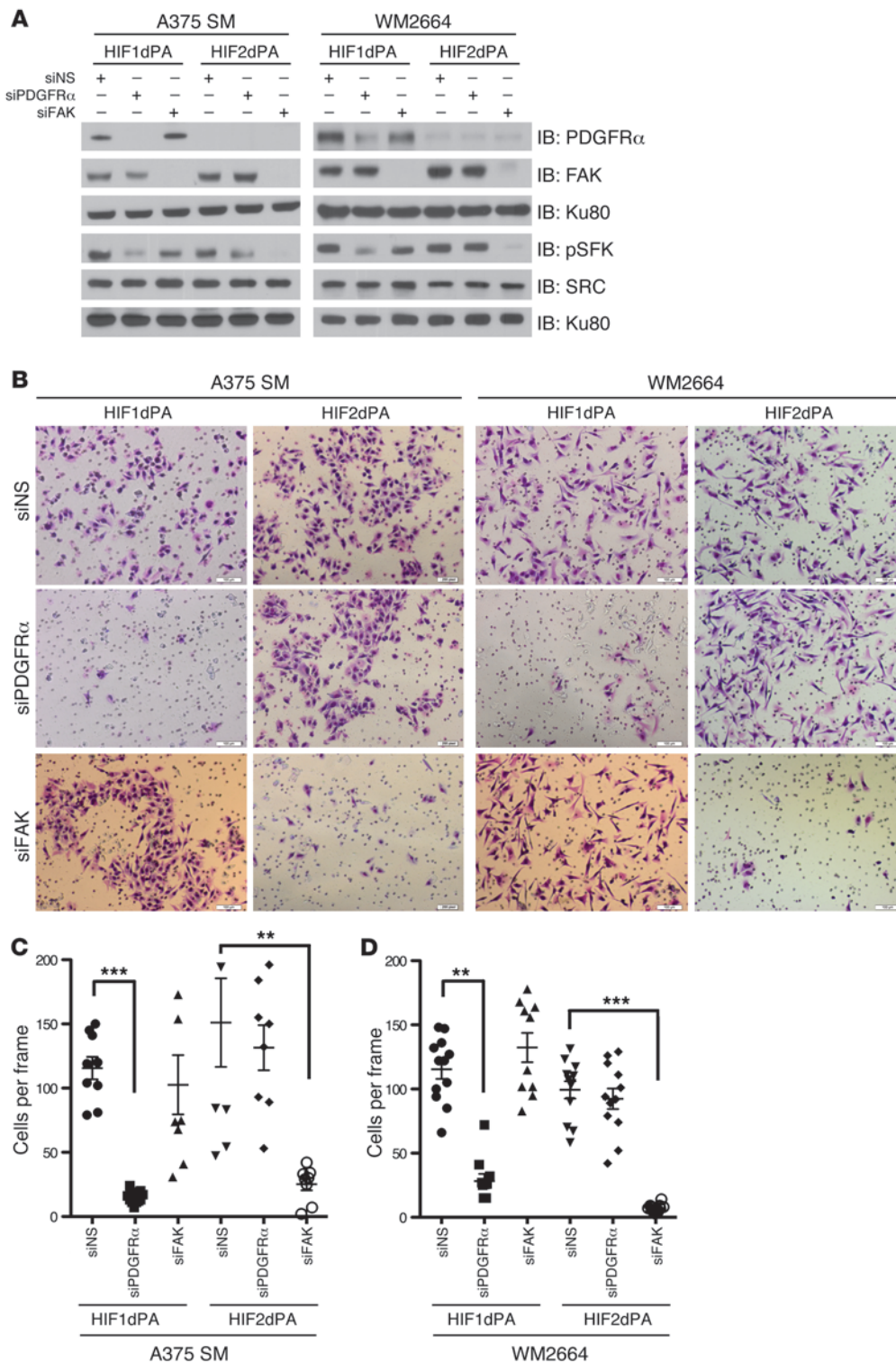
Figure 6
HIF1α and HIF2α-dependent invasion require PDGFRα and FAK, respectively. (**A**) A375 SM and WM2664 cells stably expressing EGFP, HIF1dPA, or HIF2dPA were transfected with siRNAs against PDGFRα and FAK. Whole-cell extracts were immunoblotted with the indicated antibodies. (**B**) Representative photomicrographs of A375 SM and WM2664 cells stably expressing EGFP, HIF1dPA, or HIF2dPA and transfected with indicated siRNA oligos, which have invaded through Matrigel chambers. Original magnification, ×10 magnification. (**C**) Quantification of A375 SM cells stably expressing EGFP, HIF1dPA, or HIF2dPA and transfected with siRNA oligos against either PDGFRα or FAK, which have invaded through Matrigel chambers. (**D**) Quantification of WM2664 cells stably expressing EGFP, HIF1dPA, or HIF2dPA and transfected with siRNA oligos against either PDGFRα or FAK, which have invaded through Matrigel chambers. Error bars show SEM. ***$P < 0.0005$; **$P < 0.005$.

most recently, antibodies directed at the T cell inhibitory ligand/ receptor complex PD-L1 and PD1 (36, 37). On a molecular level, HIF activation in the setting of pVHL inactivation is both necessary and sufficient for RCC tumorigenesis, and HIF appears to mediate the majority of phenotypes seen in the setting of VHL deficiency in mice (6, 31, 38, 39). Interestingly, HIF activation is a consequence

of several of the signature genetic events found in melanoma. For example, loss-of-function mutations of *PTEN* result in an Akt-dependent increase in mTOR activity and the translation of HIFα subunits (15, 18). HIF is also transcriptionally upregulated in tumors with mutant *RAS* and *BRAF* as well as in tumors overexpressing MITF (16–18, 20). Intriguingly, a recent report describes a
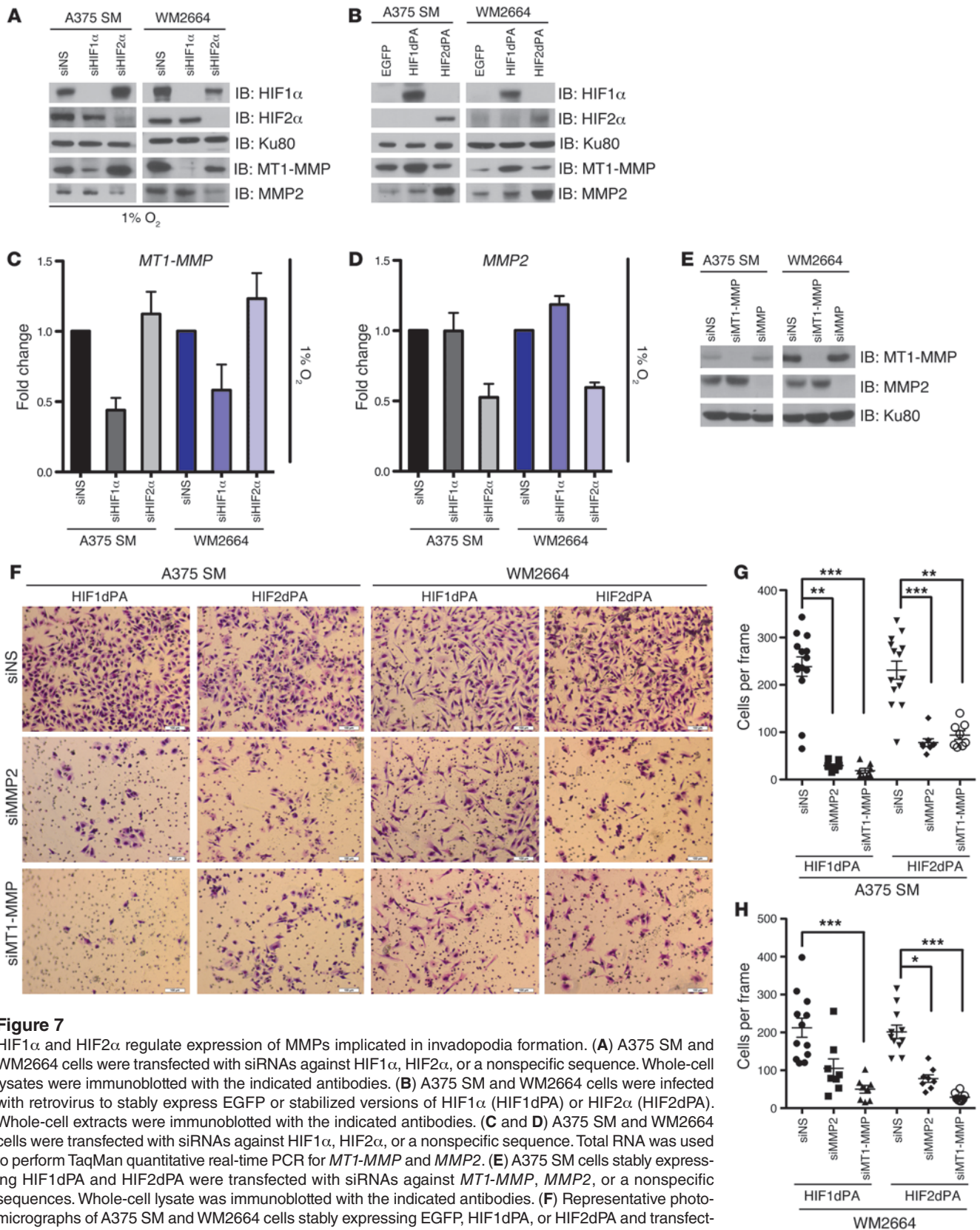
Figure 7
HIF1α and HIF2α regulate expression of MMPs implicated in invadopodia formation. (**A**) A375 SM and WM2664 cells were transfected with siRNAs against HIF1α, HIF2α, or a nonspecific sequence. Whole-cell lysates were immunoblotted with the indicated antibodies. (**B**) A375 SM and WM2664 cells were infected with retrovirus to stably express EGFP or stabilized versions of HIF1α (HIF1dPA) or HIF2α (HIF2dPA). Whole-cell extracts were immunoblotted with the indicated antibodies. (**C** and **D**) A375 SM and WM2664 cells were transfected with siRNAs against HIF1α, HIF2α, or a nonspecific sequence. Total RNA was used to perform TaqMan quantitative real-time PCR for *MT1-MMP* and *MMP2*. (**E**) A375 SM cells stably expressing HIF1dPA and HIF2dPA were transfected with siRNAs against *MT1-MMP*, *MMP2*, or a nonspecific sequences. Whole-cell lysate was immunoblotted with the indicated antibodies. (**F**) Representative photomicrographs of A375 SM and WM2664 cells stably expressing EGFP, HIF1dPA, or HIF2dPA and transfected with siRNA oligos against either *MT1-MMP* or *MMP2*, which have invaded through Matrigel chambers. Original magnification, ×10. (**G** and **H**) Quantification of A375 SM and WM2664 cells stably expressing EGFP, HIF1dPA, or HIF2dPA and transfected with siRNA oligos against *MT1-MMP* or *MMP2*, which have invaded through Matrigel chambers. Error bars show SEM. ***$P < 0.0005$; **$P < 0.005$; *$P < 0.05$.
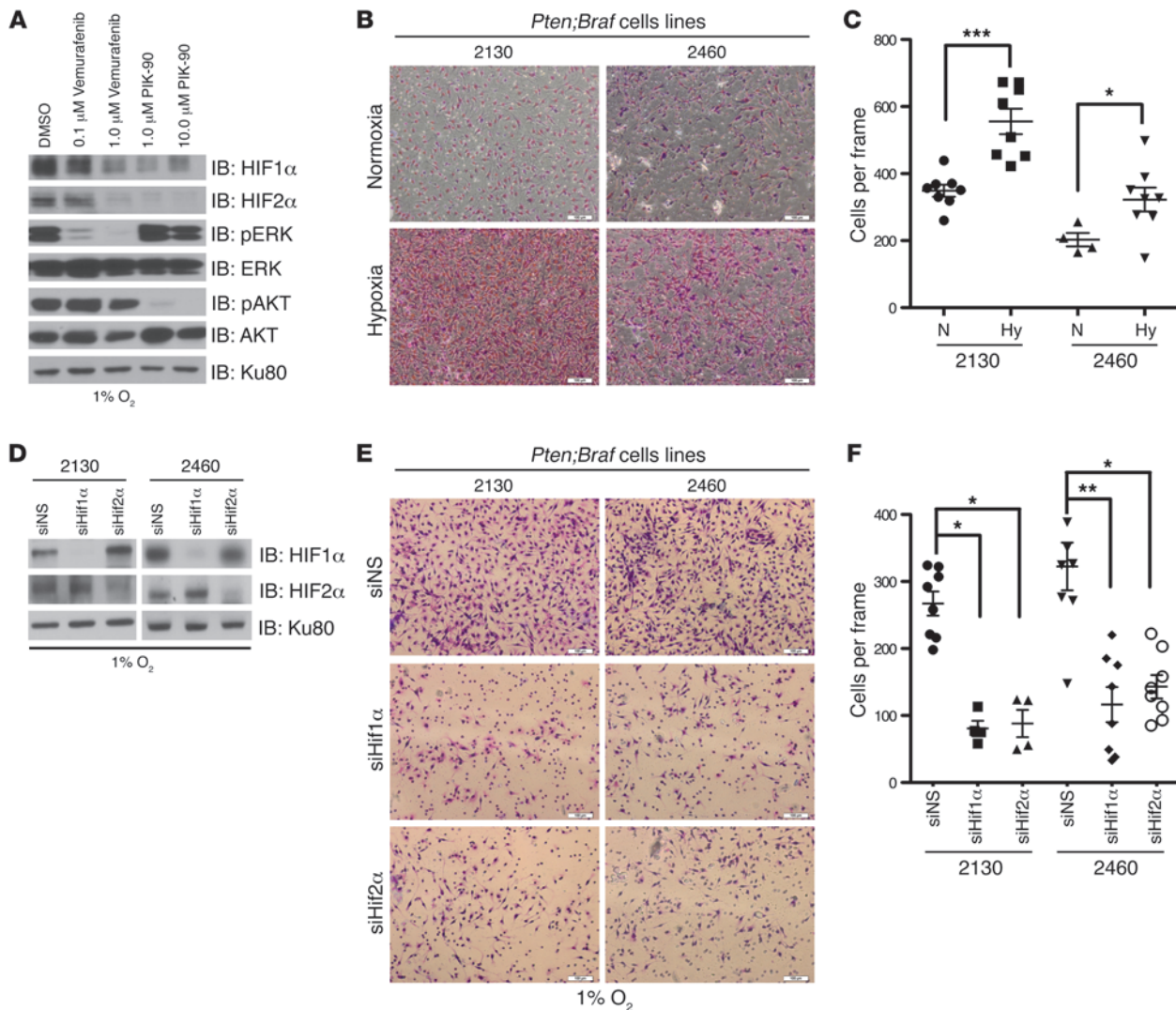
Figure 8
Knockdown of Hif1α and Hif2α reduces the hypoxia-induced invasion of cell lines derived from *Pten;Braf* melanomas. (**A**) 2460 *Pten;Braf* melanoma cells were treated with the indicated doses of vemurafenib, PIK-90, or DMSO overnight. Whole-cell lysates were immunoblotted with the indicated antibodies. (**B**) Representative photomicrographs of 2130 and 2460 *Pten;Braf* melanoma cells, which have invaded through Matrigel chambers under hypoxia or normoxia. Original magnification, ×10. (**C**) Quantification of 2130 and 2460 *Pten;Braf* melanoma cells, which have invaded through Matrigel chambers. (**D**) 2130 and 2460 *Pten;Braf* melanoma cells were transfected with siRNAs against murine *Hif1α* or *Hif2α* and immunoblotted with the indicated antibodies. (**E**) Representative photomicrographs of 2130 and 2460 *Pten;Braf* melanoma cells that were transfected with siRNAs against murine *Hif1α* or *Hif2α* and allowed to invade through Matrigel chambers under hypoxia. Original magnification, ×10. (**F**) Quantification of 2130 and 2460 *Pten;Braf* melanoma cells that were transfected with siRNAs against murine *Hif1α* or *Hif2α* and allowed to invade through Matrigel chambers under hypoxia. Error bars show SEM. ***$P < 0.0005$; **$P < 0.005$; *$P < 0.05$.

rare germline MITF mutation that predisposes to the development of melanoma, RCC, or both (40). Perhaps most interestingly, this MITF mutation, Mi-E318K, prevents its SUMOylation, enhances its chromatin occupancy, and appears to upregulate expression of genes involved in melanomagenesis and HIF1α (potential effects on HIF2α have yet to be reported). Therefore, the germline MITF mutation, Mi-E318K, appears to link two seemingly similar cancers on a molecular level, possibly through activation of HIF.

Hypoxia is associated with metastasis in many solid tumors, including melanoma. The data presented here suggest that HIF1α and HIF2α contribute to hypoxia-mediated metastatic spread through the pathways presented. PDGFRα, FAK, and SRC

are kinases and are targetable by inhibitors; indeed, inhibitors against PDGFRα (imatinib) and SRC (dasatinib) are already FDA approved and are in use for the treatment of multiple cancers. Our results imply that PDGFRα, FAK, or SRC inhibition in early stage melanoma patients may be beneficial, as these pathways are critical for hypoxia-induced melanoma cell intravasation. However, whether activation of these pathways remains necessary for the maintenance of established metastases remains to be determined.

In summary, our results establish that HIF plays an active role in the metastatic progression of melanoma and demonstrate that HIF1α and HIF2α activate independent transcriptional programs, which induce invadopodia formation and invasion

and decrease cell stiffness. We demonstrate in an autochthonous mouse model of metastatic melanoma that inactivation of Hif1α or Hif2α results in a significant reduction in metastases to regional lymph nodes, suggesting that these in vitro observations are operational in vivo (Figure 1F). This work defines 2 HIF target genes, *PDGFRA* and *FAK*, and is the first examination, to our knowledge, of the role of HIF2α in melanomagenesis. Importantly, our studies directly link hypoxia, HIF1α, and HIF2α to enhanced invadopodia formation, adding another pathologic stimulus to the list of those currently known to modify invadopodia assembly and turnover. In aggregate, our studies define HIF1α and HIF2α as intimately involved in the process of metastasis in malignant melanoma and further enforce the notion that the similarities between melanoma and RCC extend beyond mere clinical observations and rare germline genetic events.

Methods

Cell lines

Human melanoma cell lines SK Mel 24 and Sk Mel 28 were obtained from ATCC, RPMI 7951 was obtained from Lineberger Comprehensive Cancer Center Tissue Culture Facility (LCCC TCF), cell lines A375 and WM2664 were a gift from Jack Arbiser (Emory University, Atlanta, Georgia, USA), and the UACC 257 cell line was a gift from Maria Soengas (Centro Nacional de Investigaciones Oncológicas, Madrid, Spain). Cells were cultured in either DMEM with the addition of 10% FBS (Benchmark FBS; Gemini Bio-Products) and penicillin/streptomycin (Gibco; Invitrogen) (A375SM, UACC 257, WM2664, Sk Mel 24, and Sk Mel 28) or αMEM with the addition of 10% FBS and penicillin/streptomycin (RPMI 7951). Cells were incubated at 37°C under either normoxic (21% O_2 and 5% CO_2) or hypoxic (1% O_2 and 5% CO_2) conditions and medium was changed every other day.

siRNA transfections and shRNA transductions

shRNA constructs against HIF1α and HIF2α were obtained from the University of North Carolina (UNC) Lentiviral Core Facility (OpenBiosystems). Sequences are listed in Supplemental Table 1. siRNA oligos against human HIF1α and HIF2α, FAK, and PDGFRα were purchased from ABI Technologies, and siRNA oligos against murine Hif1α and Hif2α were obtained from Dharmacon. siRNA transfections were performed using the Invitrogen Lipofectamine siRNAmax Kit according to the manufacturer's instructions. Lentiviruses (pLKO) expressing shRNA against HIF1α and HIF2α were produced in 293T cells. Virus was collected after 72 hours and then placed on either A375 SM or WM2664 cells seeded at approximately 70% confluency. Puromycin selections (A375 SM at 2 μg/ml, WM2664 at 1 μg/ml) were performed starting at 48 hours.

Stable cell lines

Retroviruses (pBabe-puro) expressing stabilized versions of HIF1α or HIF2α were produced in 293T cells. Virus was collected after 72 hours and then placed on either A375 SM or WM2664 cells seeded at approximated 70% confluency. Puromycin selections (A375 SM at 2 μg/ml, WM2664 at 1 μg/ml) were performed starting at 48 hours.

Western blotting

Melanoma cell lines were grown to subconfluence in 10-cm dishes and lysed in buffer containing 200 mM Tris-HCl pH 8.0, 120 mM NaCl, and 0.5% NP-40 in the presence of protease (Roche) and phosphatase (Calbiochem) inhibitors. Whole-cell extracts (30 μg) were resolved by either 7.5% or 10% sodium dodecyl sulfate–polyacrylamide gel electrophoresis, transferred to a nitrocellulose membrane, and then probed with the specific antibodies

(Supplemental Table 2). Proteins were visualized with an enhanced chemiluminescence system from Amersham using horseradish peroxidase–conjugated anti-rabbit or anti-mouse secondary antibody (Thermo-Scientific).

Matrigel invasion

Melanoma cell lines were plated in serum-free medium overnight. Then either 50,000 or 100,000 cells were seeded into an 8-μm Matrigel chamber (BD Biosciences) with medium containing 10% FBS in the well. Cells were allowed to invade for 18–36 hours. Cells that had invaded through the Matrigel were then stained with the Siemens Staining Kit according to manufacturer's directions. Matrigel wells were then placed on a glass slide and analyzed and photographed using an Olympus IX51 microscope. Representative pictures were taken of each Matrigel well quadrant, and the number of cells that had invaded into the Matrigel was determined using ImageJ.

Invadopodia labeling and immunofluorescence

Active invadopodia were defined as colocalization of F-actin (phalloidin staining), cortactin, and degradation of fibronectin. Immunofluorescence microscopy was used to visualize the following: human fibronectin (BD Biosciences) was coupled to Alexa Fluor 568 using a protein-labeling kit (A10238; Molecular Probes). A 50-μg/ml solution was prepared in PBS and incubated on cross-linked gelatin (300 Bloom; Sigma-Aldrich) on glass coverslips. Cells were seeded onto coverslips, incubated for 18–24 hours, fixed in 4% paraformaldehyde for 20 minutes, permeabilized in PBS containing 0.5% Triton X-100 for 5 minutes, blocked in PBS containing 3% BSA for 1 hour, and then incubated with phalloidin (indicator of F actin) or antibody specific to cortactin for 2 hours. Samples were then incubated with fluorophore-conjugated secondary antibodies for 1 hour. Finally, coverslips were mounted with FluorSave reagent (Calbiochem). Experiments were observed using a LSM 710 laser scanning confocal microscope (Carl Zeiss), and images were processed using Photoshop software (Adobe Systems) and ImageJ.

Mouse colony and treatment

Animals were generated and genotyped as previously described (23) and were in a mixed background. To generate focal tumors, 6-week-old animals were treated with 1 μl of 20 mM 4-OH tamoxifen (H7904; Sigma-Aldrich) at the base of their tails. Tumor growth and survival were assessed 3 times per week by caliper measurements of tumor areas (width^2 × length)/2 [mm^2]. Mice were sacrificed once the tumor had reached a volume of 1.2 cm^3.

Mouse melanoma cell line generation

To generate mouse tumor cell lines, tumor samples were washed in PBS containing 20% penicillin/streptomycin and then dissociated in 5 ml of 0.25% trypsin for 15 minutes at 37°C. Samples were then collected with 10 ml of RPMI 1640 with 10% FBS and penicillin/streptomycin in a 15-ml conical tube and were allowed to settle for 15 minutes at room temperature. The resulting supernatant and pellet were plated on separate 10-cm plates. Medium was changed every 3 days. In order to eliminate fibroblast contamination, samples were trypsinzed with 0.05% trypsin-EDTA every week and the fibroblasts were washed off with PBS. Resulting mouse tumor cell lines were confirmed using PTEN genotyping (primers listed in Supplemental Table 2).

Real-time PCR

Total RNA was extracted from cells at 75%–90% confluency using RNeasy Mini Kit (QIAGEN) and was reverse transcribed using the ImProm-II Reverse Transcription System (Promega). Resulting cDNA was analyzed in triplicate using TaqMan 2X Universal PCR Master Mix (ABI). Relative mRNA concentrations were determined by $2^{-(Ct-Ct)}$, where Ct is the mean

threshold cycle difference after normalizing to 18S values. Primers used for PCR were purchased from ABI Technologies.

Experimental lung metastasis assay

A375 SM cells stably transduced with shRNA constructs against either HIF1α, HIF2α, or a nonspecific control were harvested by brief exposure to 0.05% trypsin EDTA solutions (Gibco; Invitrogen). Cells were washed and resuspended in Ca^{2+}- and Mg^{2+}-free HBSS (Gibco; Invitrogen). A total of 5×10^5 cells in 0.2 ml of HBSS were injected into the lateral vein of nude mice. Eight weeks later, the animals were sacrificed and the lungs were removed, washed in PBS (Cellgro), and fixed in 10% buffered formalin solution (Sigma-Aldrich) overnight to facilitate counting of surface tumor nodules.

Magnetic tweezers assay

Cultures of A375 SM cells were plated on collagen-coated glass coverslips and grown to 50%–80% confluence; 4.5 μm tosylactivated magnetic beads (Invitrogen) were conjugated with human fibronectin and incubated with the cells for 10 minutes. The 3D force microscope system was used to apply 50–100 pN of force to each bead for 5 seconds, and the resultant motion and recovery were recorded at 30 frames per second. Cells were used for as many separate fields of view as could be recorded within 1 hour. Bead position was analyzed using Video Spot Tracker software (http://cismm.cs.unc.edu) and fit to a Jeffrey's model for stiffness, as described previously (33).

TMA

Antibodies and immunohistochemistry. Rabbit polyclonal anti-HIF1α and anti-HIF2α antibodies were from Novus Biologicals and Eton Bioscience Inc., respectively.

IHC was carried out in the Bond Autostainer (Leica Microsystems Inc.). Slides were dewaxed in Bond Dewax solution (AR9222) and hydrated in Bond Wash solution (AR9590). Antigen retrieval for both antibodies was performed at 100°C in Bond-Epitope Retrieval Solution 1, pH–6.0, (AR9961) for 30 minutes for HIF1α and 40 minutes for HIF2α. Detection was performed using Bond Polymer Refine Red Detection (DS9390). Stained slides were dehydrated and coverslipped. Positive and negative controls (no primary antibody) were included for each antibody.

TMA construction. The previously described nevus to melanoma progression TMA (41) was used to stain for HIF1α and HIF2α. In addition, melanoma cases metastatic to brain, lung, and liver were obtained from UNC Hospital's surgical pathology archive to construct the UNC TMA 69A1 (UNC IRB-approved protocol 08-0242). H&E-stained slides of the selected cases were reviewed by a surgical pathologist (C.R. Miller), and representative areas of tumor and adjacent normal tissues were circled for coring. TMA block containing triplicate cores (0.6 mm) of melanoma metastases was constructed. TMA was cut into 4-micron–thick sections and placed on positively charged glass slides.

Digital imaging and image analysis. Stained TMAs were digitally imaged at ×20 magnification using the Aperio ScanScope XT (Aperio Technologies). TMA slides were de-arrayed to visualize individual cores, using TMA Lab (Aperio). Digital images were stored and evaluated by the pathologist (C.R. Miller) within the Aperio Spectrum Database using the following scoring system: 0 = neg; 1+ = cytoplasmic staining; 2+ = weak nuclear staining; 3+ = strong nuclear staining.

Statistics

Statistical analysis of percentage of living (Figure 1B) and tumor-free survival (Supplemental Figure 1D) were performed using a log-rank test. For the TMA studies (Figure 1, C and D), Wilcoxon rank-sum tests were used to compare the expression between 2 groups. All statistical analyses were carried out in R (http://cran.r-project.org/). All other statistical comparisons were done using a 2-sided t test. A P value of less that 0.05 was considered significant.

Study approval

Mice were housed and treated in accordance with protocols approved by the IACUC for animal research at the University of North Carolina.

Address correspondence to: William Y. Kim, Lineberger Comprehensive Cancer Center, University of North Carolina, CB# 7295, Chapel Hill, North Carolina 27599-7295, USA. Phone: 919.966.4765; Fax: 919.966.8212; E-mail: wykim@med.unc.edu.

1. Siegel R, Ward E, Brawley O, Jemal A. Cancer statistics, 2011: the impact of eliminating socioeconomic and racial disparities on premature cancer deaths. *CA Cancer J Clin*. 2011;61(4):212–236.
2. Flaherty KT, Hodi FS, Fisher DE. From genes to drugs: targeted strategies for melanoma. *Nat Rev Cancer*. 2012;12(5):349–361.
3. Kaelin WG, Ratcliffe PJ. Oxygen sensing by metazoans: the central role of the HIF hydroxylase pathway. *Mol Cell*. 2008;30(4):393–402.
4. Kim WY, Kaelin WG. Role of VHL gene mutation in human cancer. *J Clin Oncol*. 2004;22(24):4991–5004.
5. Semenza GL. Targeting HIF-1 for cancer therapy. *Nat Rev Cancer*. 2003;3(10):721–732.
6. Kim WY, et al. Failure to prolyl hydroxylate hypoxia-inducible factor alpha phenocopies VHL inactivation in vivo. *EMBO J*. 2006;25(19):4650–4662.
7. Raval RR, et al. Contrasting properties of hypoxia-inducible factor 1 (HIF-1) and HIF-2 in von Hippel-Lindau-associated renal cell carcinoma. *Mol Cell Biol*. 2005;25(13):5675–5686.
8. Hu C-J, Wang L-Y, Chodosh LA, Keith B, Simon MC. Differential roles of hypoxia-inducible factor 1alpha (HIF-1alpha) and HIF-2alpha in hypoxic gene regulation. *Mol Cell Biol*. 2003;23(24):9361–9374.
9. Keith B, Johnson RS, Simon MC. HIF1α and HIF2α: sibling rivalry in hypoxic tumour growth and progression. *Nat Rev Cancer*. 2012;12(1):9–22.
10. Adelman DM, Gertsenstein M, Nagy A, Simon MC, Maltepe E. Placental cell fates are regulated in vivo by HIF-mediated hypoxia responses. *Genes Dev*. 2000;14(24):3191–3203.
11. Vaupel P. Hypoxia and aggressive tumor phenotype: implications for therapy and prognosis. *Oncologist*. 2008;13(suppl 3):21–26.
12. Kozak KR, Abbott B, Hankinson O. ARNT-deficient mice and placental differentiation. *Dev Biol*. 1997;191(2):297–305.
13. Cowden Dahl KD, Robertson SE, Weaver VM,

Simon MC. Hypoxia-inducible factor regulates alphavbeta3 integrin cell surface expression. *Mol Biol Cell*. 2005;16(4):1901–1912.

14. Giatromanolaki A, et al. Hypoxia-inducible factors 1alpha and 2alpha are related to vascular endothelial growth factor expression and a poorer prognosis in nodular malignant melanomas of the skin. *Melanoma Res*. 2003;13(5):493–501.

15. Bedogni B, et al. The hypoxic microenvironment of the skin contributes to Akt-mediated melanocyte transformation. *Cancer Cell*. 2005;8(6):443–454.

16. Kumar SM, et al. Mutant V600E BRAF increases hypoxia inducible factor-1alpha expression in melanoma. *Cancer Res*. 2007;67(7):3177–3184.

17. Blancher C, Moore JW, Robertson N, Harris AL. Effects of ras and von Hippel-Lindau (VHL) gene mutations on hypoxia-inducible factor (HIF)-1alpha, HIF-2alpha, and vascular endothelial growth factor expression and their regulation by the phosphatidylinositol 3′-kinase/Akt signaling pathway. *Cancer Res*. 2001;61(19):7349–7355.

18. Sodhi A, Montaner S, Miyazaki H, Gutkind JS. MAPK and Akt act cooperatively but independently on hypoxia inducible factor-1alpha in rasV12 upregulation of VEGF. *Biochem Biophys Res Commun*. 2001;287(1):292–300.

19. Harris AL. Hypoxia — a key regulatory factor in tumour growth. *Nat Rev Cancer*. 2002;2(1):38–47.

20. Buscà R, et al. Hypoxia-inducible factor 1{alpha} is a new target of microphthalmia-associated transcription factor (MITF) in melanoma cells. *J Cell Biol*. 2005;170(1):49–59.

21. Feige E, et al. Hypoxia-induced transcriptional repression of the melanoma-associated oncogene MITF. *Proc Natl Acad Sci U S A*. 2011; 108(43):E924–E233.

22. Cheli Y, et al. Hypoxia and MITF control metastatic behaviour in mouse and human melanoma cells. *Oncogene*. 2011;31(19):2461–2470.

23. Dankort D, et al. Braf(V600E) cooperates with Pten loss to induce metastatic melanoma. *Nat Genet*. 2009;41(5):544–552.

24. Kim WY, et al. HIF2α cooperates with RAS to promote lung tumorigenesis in mice. *J Clin Invest*. 2009;119(8):2160–2170.

25. Murphy DA, Courtneidge SA. The 'ins' and "outs" of podosomes and invadopodia: characteristics, formation and function. *Nat Rev Mol Cell Biol*. 2011;12(7):413–426.

26. Yeatman TJ. A renaissance for SRC. *Nat Rev Cancer*. 2004;4(6):470–480.

27. Eckert MA, et al. Twist1-induced invadopodia formation promotes tumor metastasis. *Cancer Cell*. 2011;19(3):372–386.

28. Yang M-H, et al. Direct regulation of TWIST by HIF-1alpha promotes metastasis. *Nat Cell Biol*. 2008;10(3):295–305.

29. Gort EH, et al. The TWIST1 oncogene is a direct target of hypoxia-inducible factor-2alpha. *Oncogene*. 2008;27(11):1501–1510.

30. Hu C-J, Sataur A, Wang L, Chen H, Simon MC. The N-terminal transactivation domain confers target gene specificity of hypoxia-inducible factors HIF-1alpha and HIF-2alpha. *Mol Biol Cell*. 2007; 18(11):4528–4542.

31. Kondo K, Klco J, Nakamura E, Lechpammer M, Kaelin WG. Inhibition of HIF is necessary for tumor suppression by the von Hippel-Lindau protein. *Cancer Cell*. 2002;1(3):237–246.

32. Butcher DT, Alliston T, Weaver VM. A tense situation: forcing tumour progression. *Nat Rev Cancer*. 2009;9(2):108–122.

33. Swaminathan V, et al. Mechanical stiffness grades metastatic potential in patient tumor cells and in cancer cell lines. *Cancer Res*. 2011;71(15):5075–5080.

34. Cross SE, Jin Y-S, Rao J, Gimzewski JK. Nanomechanical analysis of cells from cancer patients. *Nat Nanotechnol*. 2007;2(12):780–783.

35. Spero RC, et al. High throughput system for magnetic manipulation of cells, polymers, and biomaterials. *Rev Sci Instrum*. 2008;79(8):083707.

36. Topalian SL, et al. Safety, activity, and immune correlates of anti-PD-1 antibody in cancer. *N Engl J Med*. 2012;366(26):2443–2454.

37. Brahmer JR, et al. Safety and activity of anti-PD-L1 antibody in patients with advanced cancer. *N Engl J Med*. 2012;366(26):2455–2465.

38. Kondo K, Kim WY, Lechpammer M, Kaelin WG. Inhibition of HIF2alpha is sufficient to suppress pVHL-defective tumor growth. *PLoS Biol*. 2003; 1(3):E83.

39. Rankin EB, et al. Inactivation of the arylhydrocarbon receptor nuclear translocator (Arnt) suppresses von Hippel-Lindau disease-associated vascular tumors in mice. *Mol Cell Biol*. 2005;25(8):3163–3172.

40. Bertolotto C, et al. A SUMOylation-defective MITF germline mutation predisposes to melanoma and renal carcinoma. *Nature*. 2011;480(7375):94–98.

41. Nazarian RM, Prieto VG, Elder DE, Duncan LM. Melanoma biomarker expression in melanocytic tumor progression: a tissue microarray study. *J Cutan Pathol*. 2010;37:41–47.